RESEARCH ARTICLE | APRIL 01 2004

Spectroscopic analysis of electrical properties in polar semiconductors with over-damped plasmons

S. Nakashima; H. Harima

J. Appl. Phys. 95, 3541–3546 (2004)
https://doi.org/10.1063/1.1655681

Spectroscopic analysis of electrical properties in polar semiconductors with over-damped plasmons

S. Nakashima
National Institute of Advanced Industrial Science and Technology, Power Electronics Research Center 1-1-1, Umezono, Tsukuba, Ibaraki, 305-8568 Japan

H. Harima
Department of Electronics and Information Science, Kyoto Institute of Technology, Matsugasaki, Kyoto, 606-8585 Japan

(Received 9 May 2003; accepted 8 January 2004)

Raman and infrared reflection spectroscopies provide us information on electronic properties in polar semiconductors. In the present work, we have employed a dielectric function including the LO phonon damping in addition to the TO phonon damping and free carrier damping, and analyzed observed spectra of *n*-type 4H–SiC crystals. The carrier density and mobility obtained from the line shape analysis as the best fit parameters are compared with those obtained using the conventional classical dielectric function. It is recognized that the LO phonon damping has a significant effect on the determination of the carrier mobility and density. © *2004 American Institute of Physics.* [DOI: 10.1063/1.1655681]

I. INTRODUCTION

Spectroscopic techniques of Raman scattering and infrared reflection have widely been used to examine electronic properties in various polar semiconductors.[1] Such spectroscopic techniques have advantages that they are nondestructive and characterization of local areas in micron scale is possible. In the infrared studies, carrier density and mobility were deduced by analyzing reflection spectra including the reststrahlen band, while in Raman scattering these quantities were obtained by analyzing the line shape of LO phonon plasmon coupled (LOPC) modes. The results of the spectroscopic analyses were often compared with those obtained mainly from Hall-effects and *C*-*V* measurements.

Carrier transport properties in semiconductors have been evaluated by both spectroscopic and electrical methods.[2–13] A number of papers reported that there was a reasonable agreement between the spectroscopic and electrical measurements. However, the carrier mobility obtained from the spectroscopic techniques was occasionally smaller than those obtained from the electrical measurements.[2,4,5,12,14,15] This discrepancy may arise from the following causes:

(i) For the determination of the drift mobility of the carriers, the Hall factor correction is required. However, this correction has often been neglected, because of the lack of information of the Hall factor, which depends on the temperature and the impurity concentration.

(ii) In the spectroscopic analyses, the effective mass of carriers was conventionally taken to be equal to the value used in the transport studies, or was chosen so that the carrier density optically determined is equal to the one determined from the transport methods. However, there remain uncertainties in equating the ''optical effective mass'' to the ''electrical transport mass.''

(iii) Furthermore, there is a question for the analyses of spectroscopic data: In most of these analyses, the classical dielectric function including the plasmon frequency ω_P, the carrier damping γ, and the TO-phonon damping Γ_T were used to obtain best fit profiles. It is anticipated, however, that the classical dielectric function is inappropriate to doped semiconductors in which the LOPC mode has a strong phononlike character and the LO phonon damping is greatly different from that of the TO phonon. Although some new formalisms of the dielectric function have been proposed, detailed analyses of spectral profile based on these modified formalisms have not been performed.

In the present study we employ a dielectric function taking into account the damping of LO phonon, and analyze the LOPC mode in *n*-type SiC crystals. SiC is chosen here as a candidate for the study of wide gap semiconductors, because its LOPC mode has a strong LO-phonon character and importance of the LO phonon damping may be actualized. The results of the spectral analyses using old and new dielectric functions are compared and discussed.

II. LINE SHAPE ANALYSIS AND DIELECTRIC FUNCTION

SiC belongs to wide band gap semiconductors in which the plasmon is over damped ($\omega_p < \gamma$, where ω_p is the plasma frequency and γ is the carrier damping), and the LO phonon frequency (around 975 cm^{-1}) is much higher than the plasma frequency except for heavily doped specimens. In this case, only the upper branch of the LOPC mode is observed at frequencies close to that of the bare LO phonon. This fact implies that the observed LOPC mode has a phononlike character predominantly and that the line shape depends critically on the LO-phonon damping. Although the LOPC mode shifts to the high frequency with increasing the carrier density in *n*-type 6H–SiC, this mode shows relatively small frequency shift compared to other polytypes, because of large carrier damping and large effective mass of electrons.[4]

This situation is a clear contrast to $III-V$ compounds like GaAs, for which the change in carrier density causes a striking shift of the LOPC modes.[16] This trend results from the small electron damping and its small effective mass.

In n-type SiC with doping levels less than 1×10^{19} cm^{-3} no appreciable broadening of the TO bands has been observed.[17] This result indicates that the TO phonon damping is almost independent of the impurity concentration. This fact is in contrast with the LO phonon damping that depends strongly on the donor concentration. The increase of the LO phonon damping with increasing impurity doping level may be due to the Fröhlich-like interaction of the LO phonon with free electrons and ionized impurities.

A. Dielectric functions

In the optical characterization, the carrier density and mobility are usually determined from the line shape fitting of Raman and infrared reflection spectra based on the classical dielectric function (CDF) including the phonon and electron contributions. The CDF that has commonly been used for zinc-blende-type crystals is written as[16,18,19]

$$\varepsilon(\omega)=\varepsilon_\infty+\frac{(\varepsilon_0-\varepsilon_\infty)\omega_{\mathrm{T}}^2}{\omega_{\mathrm{T}}^2-\omega^2-i\Gamma_{\mathrm{T}}\omega}-\frac{\varepsilon_\infty\omega_p^2}{\omega(\omega+i\gamma)}. \tag{1}$$

Here, ε_∞ is the optical dielectric constant, ω_{T} (ω_{L}) is the uncoupled TO (LO) phonon frequency, $\Gamma_{\mathrm{T}}(\gamma)$ is the damping rate of TO phonon (plasmon), and ω_{p} is the plasmon frequency given by the carrier density n and the effective mass of electrons m^*

$$\omega_p=\sqrt{\frac{4\pi ne^2}{\varepsilon_\infty m^*}}. \tag{2}$$

Here, e is the electron charge, and only the electron plasma is considered. The carrier mobility is deduced from m^* and γ using

$$\mu=\mathrm{e}/\mathrm{m}^*\gamma. \tag{3}$$

It is assumed in Eq. (1) that the phonon and electron systems are independent and that the contributions from the two systems are additive. This equation is rewritten as

$$\frac{\varepsilon(\omega)}{\varepsilon_\infty}=\frac{\omega_{\mathrm{L}}^2-\omega^2-i\Gamma_{\mathrm{T}}\omega}{\omega_{\mathrm{T}}^2-\omega^2-i\Gamma_{\mathrm{T}}\omega}-\frac{\omega_p^2}{\omega(\omega+i\gamma)}. \tag{4}$$

It is easily understood from the generalized Lyddane–Sacks–Teller (LST) relation[20–23] that in Eq. (4) the damping of the LO phonon is taken to be the same as that of the TO phonon. This is not the case for doped semiconductors, however, because in addition to the phonon–phonon interaction there are the interactions of the LO phonon with free electrons, ionized impurities and dipoles due to D-A pairs.

We shall take the following form of modified classical dielectric function (m-CDF) to analyze relatively highly doped SiC crystals:

$$\frac{\varepsilon_{\mathrm{M}}(\omega)}{\varepsilon_\infty}=\frac{\omega_{\mathrm{L}}^2-\omega^2-i\Gamma_{\mathrm{L}}\omega}{\omega_{\mathrm{T}}^2-\omega^2-i\Gamma_{\mathrm{T}}\omega}-\frac{\omega_p^2}{\omega(\omega+i\gamma)}, \tag{5}$$

where $\Gamma_{\mathrm{L}}(\Gamma_{\mathrm{T}})$ is the damping of the LO(TO) phonon. This formula has been used for analysis of infrared reflection[24–26] and Raman spectra.[27,28] The first term of Eq. (5) (phonon part) has the form of the generalized LST relation. This equation is reduced to Eq. (4) when $\Gamma_{\mathrm{L}}=\Gamma_{\mathrm{T}}$.

A different form of dielectric function obtained by extending the generalized LST relation to systems containing plasmons[29–32] is

$$\varepsilon_{\mathrm{k}}(\omega)=\frac{\varepsilon_\infty(\omega^2-\omega_1^2+i\gamma_1\omega)(\omega^2-\omega_2^2+i\gamma_2\omega)}{\omega(\omega+i\gamma_{\mathrm{p}})(\omega^2-\omega_{\mathrm{T}}^2+i\Gamma_{\mathrm{T}}\omega)}, \tag{6}$$

where $\omega_{1,2}$ are the frequencies of the lower and upper branches of the LO-phonon plasmon coupled mode, and $\gamma_{1,2}$ are their damping constants. Spectral analyses using the Lindhard-Mermin dielectric function have also been reported by several authors.[33–35] Infrared spectra of GaAs and CdTe were well fitted by using Eq. (6).[31] From the fitting the parameters ω_1, ω_2, γ_1, γ_2, γ_{p}, and γ_{t} were determined. However, since there is no theoretical treatment connecting the damping constants γ_1 and γ_2 to measurable physical quantities, Eq. (6) has not widely been used for spectroscopic analysis.

B. Raman scattering

Raman scattering intensity by use of the dielectric function Eq. (5) is given by

$$W(\omega)=S[\mathrm{n}(\omega)+1]A_1(\omega)\mathrm{Im}\left(\frac{-1}{\varepsilon_{\mathrm{M}}(\omega)}\right), \tag{7}$$

where

$$A(\omega)=F_1(\omega)-\frac{\varepsilon_1(\omega)}{\varepsilon_2(\omega)}F_2(\omega). \tag{8}$$

$$\varepsilon_{\mathrm{M}}(\omega)=\varepsilon_1(\omega)+\varepsilon_2(\omega). \tag{9}$$

$$\varepsilon_1(\omega)=\varepsilon_\infty\left[\frac{(\omega_{\mathrm{L}}^2-\omega^2)(\omega_{\mathrm{T}}^2-\omega^2)+\omega^2\Gamma_{\mathrm{T}}\Gamma_{\mathrm{L}}}{(\omega_{\mathrm{T}}^2-\omega^2)^2+(\omega\Gamma_{\mathrm{T}})^2}-\frac{\omega_p^2}{\omega^2+\gamma^2}\right]. \tag{10}$$

$$\varepsilon_2(\omega)=\varepsilon_\infty\left[\frac{\omega\Gamma_{\mathrm{T}}(\omega_{\mathrm{L}}^2-\omega^2)-\omega\Gamma_{\mathrm{L}}(\omega_{\mathrm{T}}^2-\omega^2)}{(\omega_{\mathrm{T}}^2-\omega^2)^2+(\omega\Gamma_{\mathrm{T}})^2}+\frac{\omega_{\mathrm{p}}^2\gamma}{\omega(\omega^2+\gamma^2)}\right]. \tag{11}$$

The exact forms of the functions F_1 and F_2 are given by the followings:[28]

$$F_1=\mathrm{Re}(F)=1+2C\frac{\omega_T^2}{\omega_L^2-\omega_T^2}\frac{(\omega_L^2-\omega_T^2)(\omega_T^2-\omega^2)+\omega^2\Gamma_T(\Gamma_L-\Gamma_T)}{(\omega_T^2-\omega^2)^2+(\omega\Gamma_T)^2}-\frac{C^2\omega_T^4}{(\omega_L^2-\omega_T^2)^2}$$
$$\times\left\{\left[\frac{(\omega_L^2-\omega_T^2)(\omega_T^2-\omega^2)+\omega^2\Gamma_T(\Gamma_L-\Gamma_T)}{(\omega_T^2-\omega^2)^2+(\omega\Gamma_T)^2}\right]\left[1-\frac{\omega_p^2}{\omega^2+\gamma^2}\right]-\frac{\omega_p^2\gamma\Gamma_T(\omega_L^2-\omega_T^2)-\omega_p^2\gamma(\Gamma_L-\Gamma_T)(\omega_T^2-\omega^2)}{(\omega^2+\gamma^2)[(\omega_T^2-\omega^2)^2+(\omega\Gamma_T)^2]}\right\}, \tag{12}$$

and

$$F_2(\omega)=\mathrm{Im}(F)=2C\frac{\omega_T^2}{\omega_L^2-\omega_T^2}\frac{\omega\Gamma_T(\omega_L^2-\omega_T^2)-\omega(\Gamma_L-\Gamma_T)(\omega_T^2-\omega^2)}{(\omega_T^2-\omega^2)^2+(\omega\Gamma_T)^2}+\frac{C^2\omega_T^4}{(\omega_L^2-\omega_T^2)^2}$$
$$\times\left\{\frac{\omega_p^2\gamma(\omega_L^2-\omega_T^2)(\omega_T^2-\omega^2)+\omega^2\omega_p^2\gamma\Gamma_T(\Gamma_L-\Gamma_T)}{\omega(\omega^2+\gamma^2)[(\omega_T^2-\omega^2)^2+(\omega\Gamma_T)^2]}\right.$$
$$\left.+\left(1-\frac{\omega_p^2}{\omega^2+\gamma^2}\right)\frac{\omega\Gamma_T(\omega_L^2-\omega_T^2)-\omega(\Gamma_L-\Gamma_T)(\omega_T^2-\omega^2)}{(\omega_T^2-\omega^2)^2+(\omega\Gamma_T)^2}\right\}. \tag{13}$$

where C is the Faust–Henry coefficient.[36]
When we put $\Gamma_L=\Gamma_T$, Eqs. (12) and (13) are reduced to conventional expression.[2,19]

We have fitted Eq. (7) to observed LOPC mode profiles using ω_p, γ, and Γ_L as adjustable parameters. We need the other material parameters, ω_L, ω_T, ε_∞, C, m^* in addition to ω_p γ, Γ_L, and Γ_T. The values of ω_p, γ, and Γ_L are adjusted for all our calculations and ω_T, ε_∞, C, m^* are taken from Ref. 4.

C. Infrared reflection

The reflectivity R of a semi-infinite medium at normal incidence is given by

$$R=\frac{(n-1)^2+k^2}{(n+1)^2+k^2}, \tag{14}$$

where n and k are the refractive and absorption indices, respectively. n and k are related to the complex dielectric function $\varepsilon_M(\omega)$,

$$\varepsilon_M(\omega)=\varepsilon_1+i\varepsilon_2=\tilde{n}^2=(n-ik)^2. \tag{15}$$

ε_1 and ε_2 are given by Eqs. (10) and (11), respectively.

III. ANALYSIS OF RAMAN AND INFRARED REFLECTION SPECTRA

SiC has a large number of polytypes. All SiC polytypes but 3C–SiC are uniaxial crystals and have a number of TO and LO phonon modes. For 4H– and 6H–SiC, E_1 and A_1 type modes are both infrared and Raman active and show the LO–TO splitting. Since there are an E_1 and an A_1 mode in these polytypes, the approach for the zinc-blende structure can be applied to each mode in these polytypes.

Raman spectra were measured at room temperature by a double monochromator with $f=1.0$ m equipped with a microscope and a liquid nitrogen cooled charge-coupled device detector. The spectral resolution was 0.2 cm^{-1}. The 488 nm line of an Ar ion laser was used. Infrared reflection spectra were measured with a Fourier transform infrared spectrometer with a microscope and a HgCdTe (MCT) detector cooled to liquid nitrogen temperature.

The fits were made by means of a nonlinear least-squares-fit computer program. The program adjusted these fitting parameters in order to minimize χ^2. When the fitting was proceeded without any constraints on the parameters, the least-squares fit occasionally provided adjustable parameters beyond physically realizable limits, even though the minimal χ^2 was obtained. This situation often occurs for spectra with poor signal–to–noise ratios. In this case, the fitting seemed to lead to smaller phonon damping, and lager carrier density and damping. This trend may arise from the fact that for the distortion and broadening of the LOPC mode the LO phonon damping plays almost the same role as that of the free carrier damping, and that the peak shift of the LOPC mode due to the increase of the carrier density is compensated by the increase of the carrier damping. In order to obtain a reasonable carrier damping the fitting under a suitable constraint on the LO phonon damping will be effective.

A. Analysis of Raman spectra

We have conducted the line shape analysis of the LOPC modes in 4H–SiC crystals with various carrier concentrations. Figure 1 shows the observed Raman spectrum of a crystal with a carrier density of $\sim 4\times10^{18}$ cm^{-3}. The best fit curves for the m-CDF and CDF models are also shown in Figs. 1(a) and 1(b), respectively. The two models give almost the same curves except for the slight deviation in the low frequency region of the LOPC mode, whereas the m-CDF model provides slightly lower carrier density and damping than the CDF model.

In Fig. 2 we show an experimental LOPC band and least-squares fits calculated using the m-CDF and CDF models for sample with $n\sim9\times10^{17}$ cm^{-3}. The two models provide almost the same line shapes that are in excellent agree-

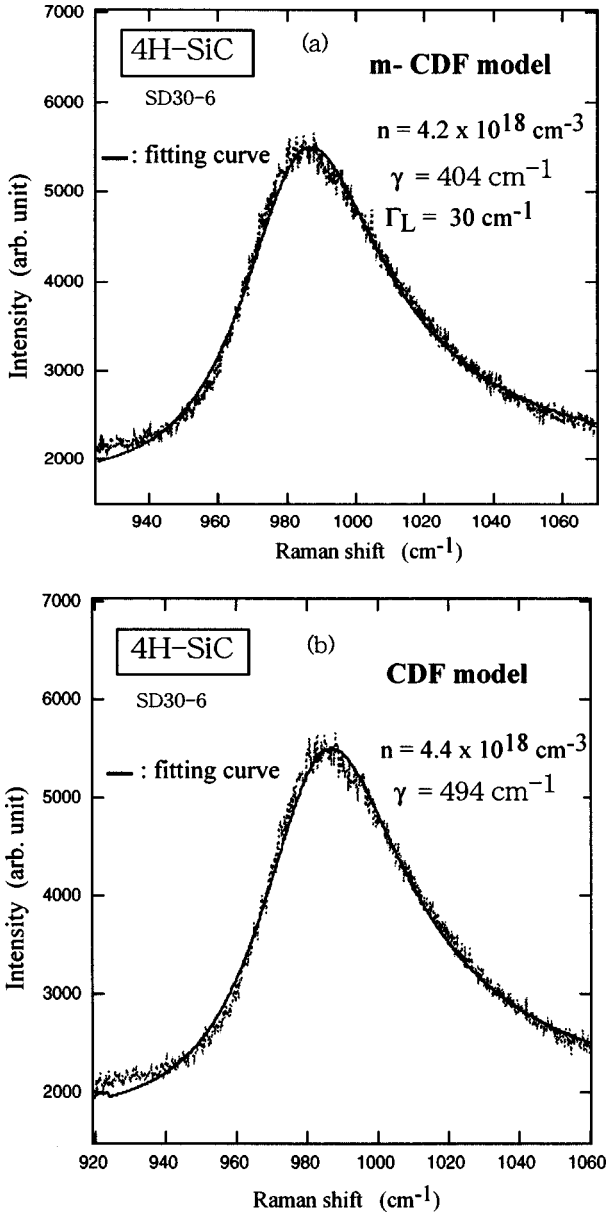

FIG. 1. Experimental LOPC band (thin solid line) and least-squares fit (solid line) for a sample with a carrier concentration of $\sim 4\times 10^{18}$ cm^{-3}, (a) the fit by use of the *m*-CDF and (b) the fit by use of the CDF. The fit is calculated with parameters $\omega_T = 783$ cm^{-1}, $\omega_L = 964$ cm^{-1}, for (a) $\Gamma_L = 30$ cm^{-1}, $\Gamma_T = 2.5$ cm^{-1}, and (b) $\Gamma_T = 28$ cm^{-1}.

ment with the observed spectrum, while the two models give different values for γ. The best fit value of γ for the *m*-CDF ($\gamma = 291$ cm^{-1}) is also smaller than that of the CDF model ($\gamma = 405$ cm^{-1}) as depicted in this figure.

The results of the simulation for samples with other carrier densities showed that the line shape of the LOPC mode is not much sensitive to the TO-phonon damping, but sensitive to the damping of the LO phonon and carriers. For highly doped specimens, the fit to experimental spectra was better for the *m*-CDF than for the CDF.

B. Analysis of infrared spectra

A reflection spectrum of a 4H–SiC crystal with a carrier concentration of 1.6×10^{18} cm^{-3} is shown in Fig. 3. The

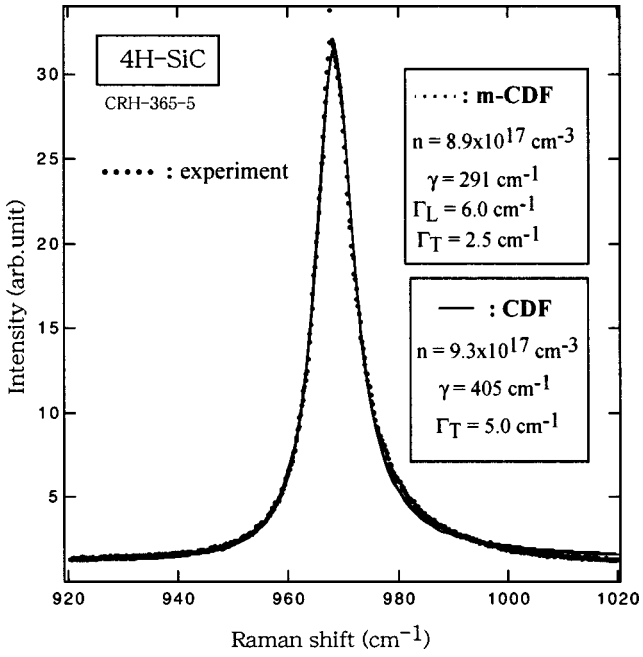

FIG. 2. Experimental LOPC band (circles) and least-squares fits by use of the *m*-CDF (dotted line) and CDF (solid line). The fit by use of the two models are almost the same. We cannot distinguish them at a glance. However, the two models provide different values of γ; $\gamma = 291$ cm^{-1} for the *m*-CDF and $\gamma = 405$ cm^{-1} for the CDF

solid line is the least-squares fit using the *m*-CDF, which shows excellent agreement with the experimental result. The inset is the expanded view of the observed reststrahlen band and a comparison of the fits between the *m*-CDF and CDF. When the *m*-CDF is used, the best fit value of the LO phonon damping is different from that of the TO phonon. The

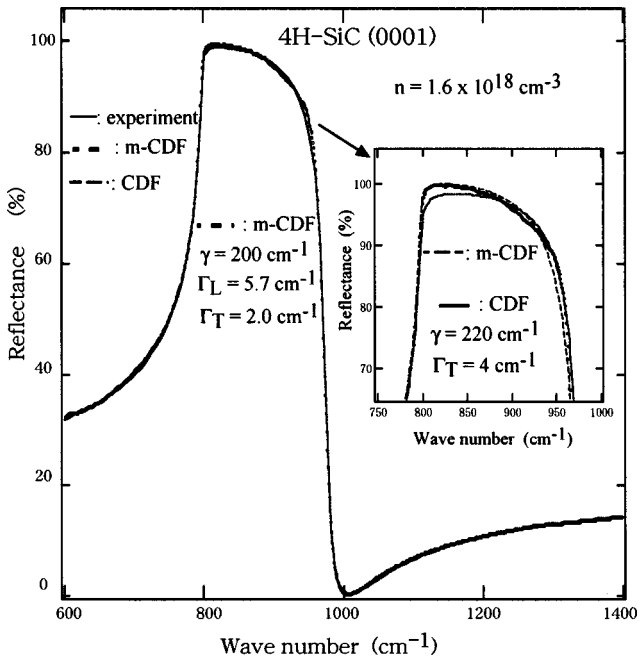

FIG. 3. Experimental reflectance (circles) and least-squares fit for sample with $n = 1.6\times 10^{18}$ cm^{-3} using the *m*-CDF. The best fit parameters are shown in the figure. The fit is calculated with $\omega_T = 783$ cm^{-1} and $\omega_L = 964.2$ cm^{-1}. The inset is the expanded view of the reststrahlen band.

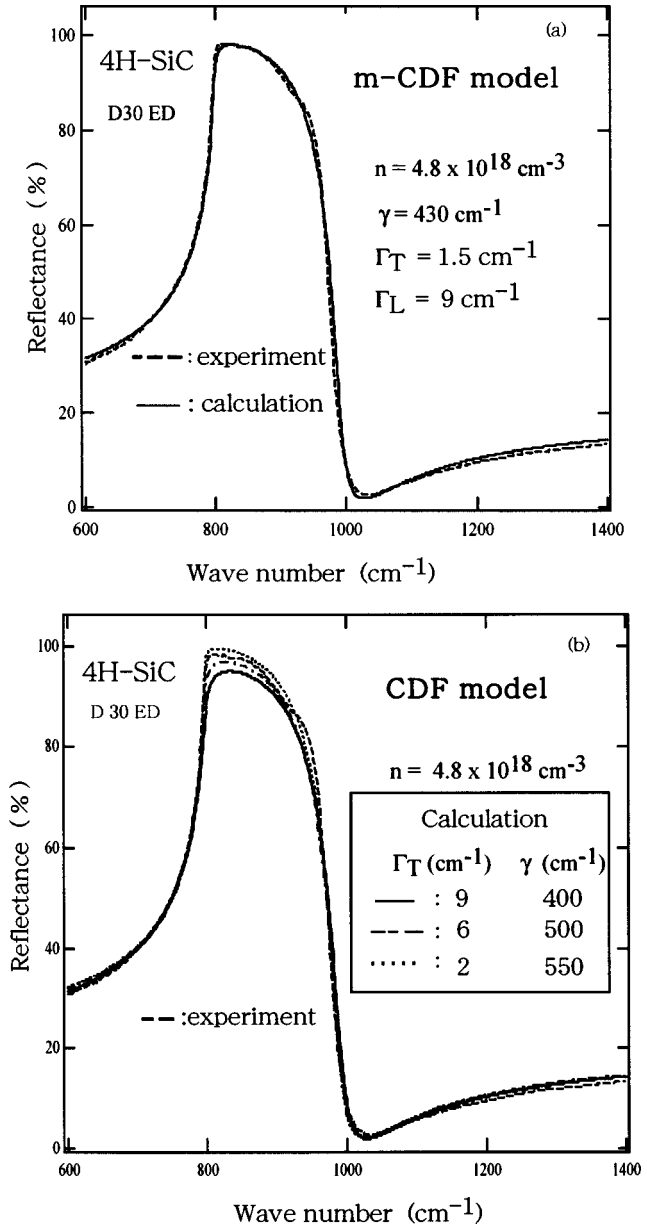

FIG. 4. (a) Experimental reflectance (broken line) and calculated fit (solid line) for a sample with $n=4.8\times10^{18}$ cm^{-3}. The best fit parameters are: $\gamma=430$ cm^{-1}, $\Gamma_L=9$ cm^{-1}, and $\Gamma_T=1.5$ cm^{-1}. (b) Calculated curves for three sets of γ and Γ for the CDF model.

reflection profile in the vicinity of ω_T is sensitive to the value of the TO-phonon damping. The spectrum calculated using the CDF with $\Gamma_T=\Gamma_L$ deviates from the experimental profile at ω_T. The increase of the carrier damping and LO-phonon damping allows rounding off the reflection edge in the vicinity of ω_L without the change of the profile at ω_T.

Figure 4(a) shows fits based on the *m*-CDF for a sample with carrier concentration of 4.8×10^{18} cm^{-3}. In Fig. 4(b) we show calculated curves for three sets of parameters γ and Γ using the CDF model. These sets of parameters give spectra that deviate from the experimental result in vicinity of ω_L or ω_T. Fitting by the CDF yielded phonon dampings larger than the TO phonon damping obtained by the *m*-CDF. In order to reproduce the rounded edge profiles at ω_L with the (CDF) model, the carrier damping larger than the *m*-CDF is needed. When the carrier damping γ obtained by the *m*-CDF was employed for the fitting of the profile in the vicinity of ω_L, a larger phonon damping was necessary at the expense of the fit at ω_T as shown in Fig. 4. Figures 3 and 4 reveal that when the CDF is used it is difficult to reproduce the whole reflection spectra both in the vicinity of ω_T and ω_L, especially for highly doped SiC.

C. LO phonon damping

In the fitting of Raman and infrared spectra using the CDF we assumed that the TO phonon damping was frequency dependent and that it varied with the carrier concentration. However, recent experiments have shown that the TO-phonon damping is almost independent of the carrier density up to $\sim1\times10^{19}$ cm^{-3}.[16] In the fitting using the *m*-CDF we can take Γ_T as a constant independent of the carrier density. This approach implies that the introduction of the LO-phonon damping is physically reasonable.

As stated before, one sometimes encounters a situation that the best fit parameters exceed a physically reasonable range. In this case it is effective to carry out the fitting under the assumption that Γ_L depends on the carrier density and is restricted within a certain range. More recently, we have measured the LOPC mode in doped 6H–SiC crystals with a carrier concentration gradient from 4×10^{17} to 2×10^{18} cm^{-3} and deduced the LO-phonon damping from the line shape analysis.[28] It was found that the LO-phonon damping obtained from the fitting is approximated by the following equation:

$$\Gamma_L\sim\Gamma_0+an, \tag{16}$$

where Γ_0 is the LO phonon damping in pure crystals, and arises from the phonon–phonon interaction, *n* is the free carrier concentration, and *a* is the proportional constant ranging in $a=0.2\sim0.4\times10^{-17}$ cm^{-1}/cm^3 for 4H–SiC bulk crystals. The second term in Eq. (16) may arise from the interaction of the LO phonon with free carriers and ionized impurities.[37] The phonon damping in impurity doped materials was studied by Surovtsev *et al.*,[38] who showed that the phonon damping varied linearly with the impurity concentration as Eq. (16). Our simulation suggested that the fitting under a restriction of Γ_L is efficient to obtain reasonable carrier damping constants.

It should be noted that the relation Eq. (16) will not hold in heavily doped crystals for which the plasma frequency is comparable to, or larger than the bare LO phonon frequency. In this case, the coupling between phonon and carrier systems is strong and the concept that there are two independent energy decay channels as described by Eqs. (4) and (5) will not be valid. In this case, it will be desirable to use the generalized LST relation Eq. (6) instead of Eq. (5).

IV. CONCLUSIONS

We examined Raman spectra of the LOPC mode and infrared reflection spectra of *n*-type 4H–SiC crystals using the modified dielectric function which included both the TO

and LO phonon damping. The carrier density and mobility were determined by fitting the theoretical curves to the experimental spectra.

The profile simulation indicated that theoretical reflection profiles using the modified classical dielectric function (m-CDF) reproduced the experimental results better than the classical dielectric function (CDF). Concerning the Raman scattering analysis, the fitting using the m-CDF and CDF reproduces well the experimental spectral profiles, but the fitting using the m-CDF has a trend to give smaller carrier density compared with that of the CDF. The m-CDF mobility was closer to the values obtained from Hall measurements.

In the present work, our analysis is limited to SiC crystals, but it could be applied by using the m-CDF to other polar semiconductors having plasmon and phonon systems with heavily damped natures.

ACKNOWLEDGMENTS

A part of this work is supported by METI partly through NEDO. One of the authors (S.N) would like to thank Dr. Fukasawa for helpful comments.

[1] S. Perkowitz, *Optical Characterization of Semiconductors* (Academic Press, London, 1993).
[2] H. Yugami, S. Nakashima, and A. Mitsuishi, J. Appl. Phys. **61**, 354 (1987).
[3] M. Ramsteiner, J. Wagner, P. Hiesinger, K. Köhler, and U. Rössler, J. Appl. Phys. **73**, 5023 (1993).
[4] H. Harima, S. Nakashima, and T. Uemura, J. Appl. Phys. **78**, 1996 (1995).
[5] G. Irmer, W. Siegel, G. Kühnel, J. Monecke, F. M. M. Yauoka, B. H. Bairamov, and V. V. Toprov, Semicond. Sci. Technol. **6**, 1072 (1991).
[6] M. Chafai, A. Jaouhari, A. Torres, R. Anton, E. Martin, J. Jimenez, and W. C. Mitchel, J. Appl. Phys. **90**, 5211 (2001).
[7] H. Harima, J. Phys.: Condens. Matter **14**, R967 (2002).
[8] B. H. Bairamov, A. Heinrich, G. Irmer, V. V. Toporov, and E. Ziegler, Phys. Status Solidi B **119**, 227 (1983).
[9] W. G. Spitzer, D. A. Kleinman, and D. Walsh, Phys. Rev. **113**, 133 (1959).
[10] R. T. Holm, J. W. Gibson, E. D. Palik, J. Appl. Phys. **48**, 212 (1977).
[11] A. Mezerreg, C. Llinares, and A. Montaner, Phys. Status Solidi B **169**, 121 (1992).
[12] Z.-F. Li, W. Lu, Z. H.-J. Ye, Z.-H. Chen, X.-Z. Yuan, H.-F. Dou, S.-C. Shen, G. Li, and S. J. Chua, J. Appl. Phys. **86**, 2691 (1999).
[13] C. Julien, I. Samaras, O. Gorochov, and A. M. Ghorayeb, Phys. Rev. B **45**, 13390 (1992).
[14] C. Pickering, J. Phys. D **16**, 213 (1983).
[15] T. Kozawa, T. Kachi, H. Kano, Y. Taga, M. Hashimoto, N. Koide, and K. Manabe, J. Appl. Phys. **75**, 1098 (1994).
[16] M. V. Klein, in *Light Scattering in Solids*, Vol. 1, edited by M. Cardona (Splinger, Berlim, 1975).
[17] S. Nakashima, K. Matsuda, M. Yoshikawa, S. Nishizawa, and N. Oyanagi, *Proceedings of 18th International Conference on Raman spectroscopy*, Budapest, 2002, edited by J. Mink, G. Jalsovszky, and G. Keresztury (Wiley, New York, 2002), p. 509.
[18] D. T. Hon and W. L. Faust, Appl. Phys. (N.Y.) **2**, 241 (1973).
[19] G. Irmer, V. V. Toporov, B. H. Bairamov, and J. Monecke, Phys. Status Solidi B **119**, 595 (1983).
[20] T. Kurosawa, J. Phys. Soc. Jpn. **16**, 1298 (1961).
[21] A. S. Chaves and S. P. S. Porto, Solid State Commun. **13**, 865 (1973).
[22] T. Takahashi, Phys. Rev. B **11**, 1636 (1975).
[23] R. J. Gonzalez and R. Zallen, and H. Berger, Phys. Rev. B **55**, 7014 (1997).
[24] J.-F. Baumard and F. Gervais, Phys. Rev. B **15**, 2316 (1977).
[25] F. Gervais, Phys. Rev. B **23**, 6580 (1981).
[26] J. M. Miljkovic, N. Lomcevic, Z. V. Popovic, W. Koenig, and V. N. Nikiforov, Phys. Status Solidi B **193**, 43 (1996).
[27] E. Neyret, G. Ferro, S. Juillaguet, J. M. Bluet, C. Jaussaud, J. Camassel, Mater. Sci. Eng., B **61–62**, 253 (1999).
[28] S. Nakashima and H. Harima J. Appl. Phys. **95**, 3547 (2004).
[29] A. A. Kukharskii, Fiz. Tverd. Tela (Leningrad) **14**, 1744 (1972) [Sov. Phys. Solid State **14**, 1501 (1972)].
[30] A. A. Kukharskii, Solid State Commun. **13**, 1761 (1973).
[31] S. Perkowitz and R. H. Thorland, Solid State Commun. **16**, 1093 (1975).
[32] B. H. Bairamov, I. P. Ipatova, V. A. Milorava, V. V. Toporov, K. Naukkarien, T. Toumi, G. Irmer, and J. Monecke, Phys. Rev. B **38**, 5722 (1988).
[33] M. Ramsteiner, J. Wagner, P. Hiesinger, K. Köhler, and U. Rössler, J. Appl. Phys. **73**, 5023 (1993).
[34] R. Cuscó, L. Artús, S. Hernández, J. Ibáñez, and M. Hopkinson, Phys. Rev. B **65**, 035 210 (2001).
[35] L. Artús, R. Cuscó, J. Ibáñez, N. Blanco, and G. González-Díaz, Phys. Rev. B **60**, 5456 (1999).
[36] W. L. Faust and C. H. Henry, Phys. Rev. Lett. **17**, 1265 (1966).
[37] B. K. Ridley and R. Gupta, Phys. Rev. B **43**, 4939 (1991).
[38] N. V. Surovtsev, I. N. Kupriyanov, V. K. Malinovski, V. A. Gusev, and Yu. N. Pal'yanov, J. Phys.: Condens. Matter **11**, 4767 (1999).